

A microscopic image showing various biological cells, possibly bacteria or yeast, with blue highlights indicating specific components or structures. The cells are of different shapes and sizes, some appearing as small spheres and others as larger, more complex structures. The background is a light, neutral color, making the blue highlights stand out.

BIO VERRES

Pierre WEISS

Equipe REGOS – RMeS lab U1229

Nantes

Pierre.weiss@univ-nantes.fr

Le squelette

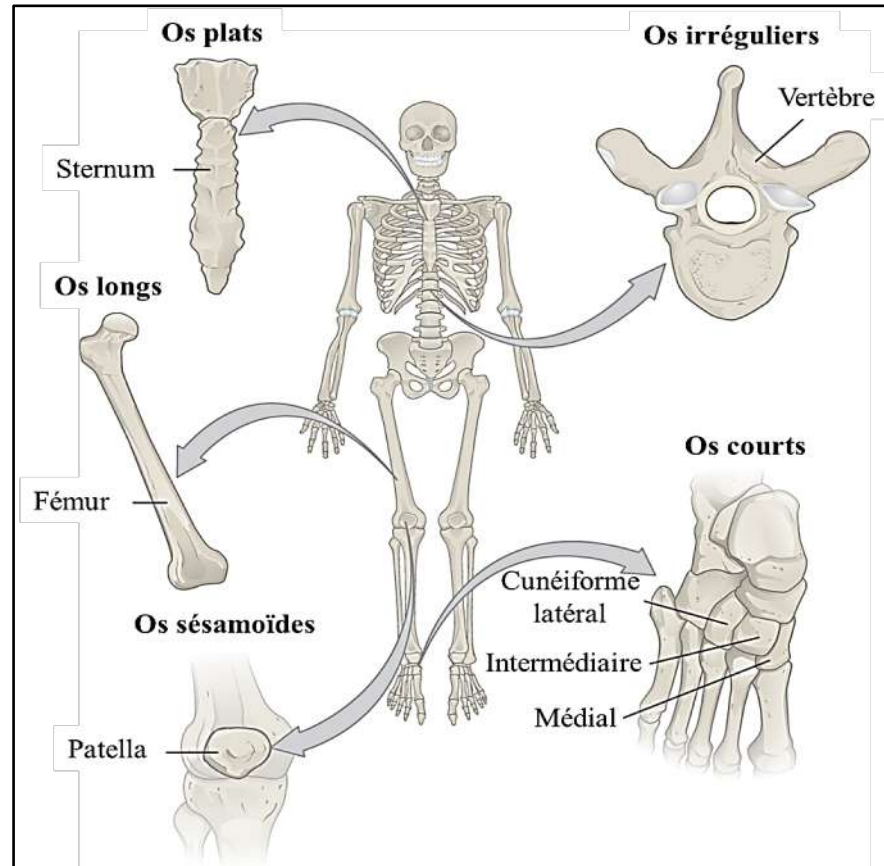


Figure 1 : Classification à cinq catégories des pièces osseuses du squelette humain. Modifié d'après [16].

Constitution du tissu osseux

Structure des os plats

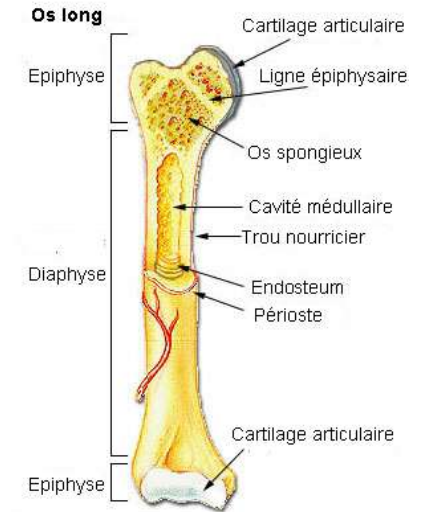
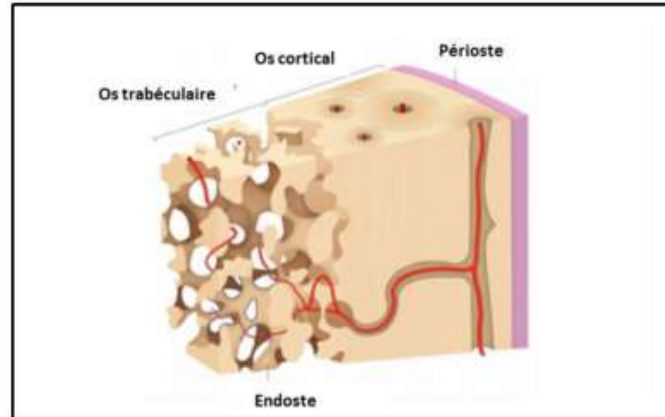
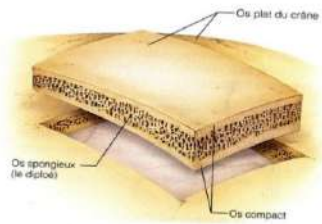


Figure 1 : schéma de l'architecture du tissu osseux (5).
Morrison SJ, Vol. 505,. Nature; 2014

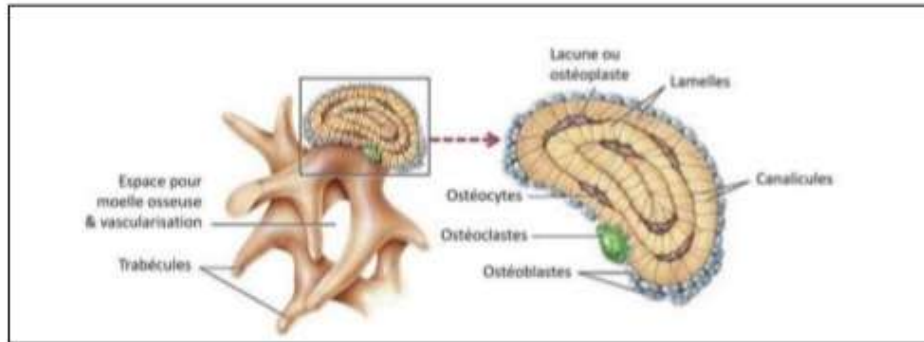


Figure 3 : Représentation schématique de l'os trabéculaire (8).

Wang X, Biomaterials. 2016

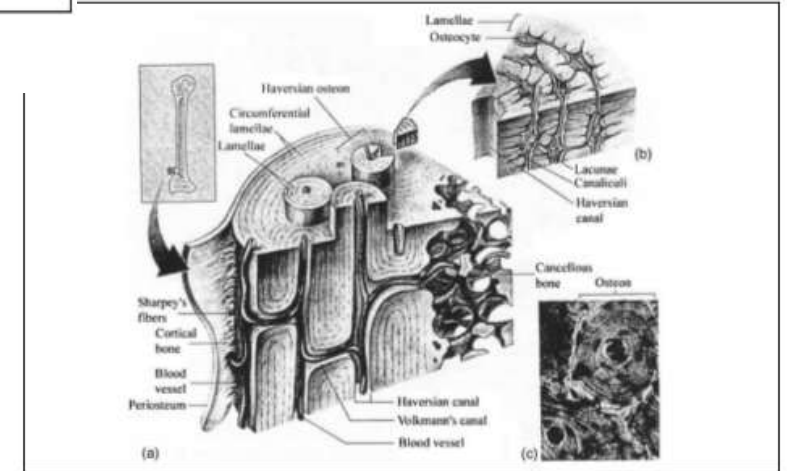


Figure 2 : Structure microscopique de l'os cortical (A) représentation 3D de l'os cortical, (B) coupe du système Haversien (C) photomicrographie du système Haversien (7).

Doblaré M, Engineering Fracture Mechanics. 2004

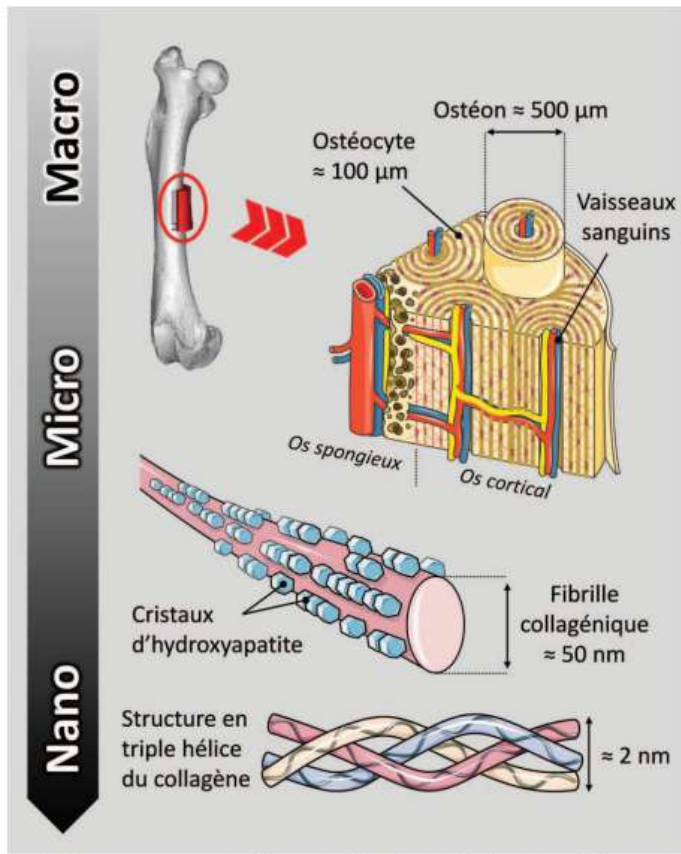


Schéma des différentes composantes de l'os naturel à différentes échelles (courtoisie banque d'images)

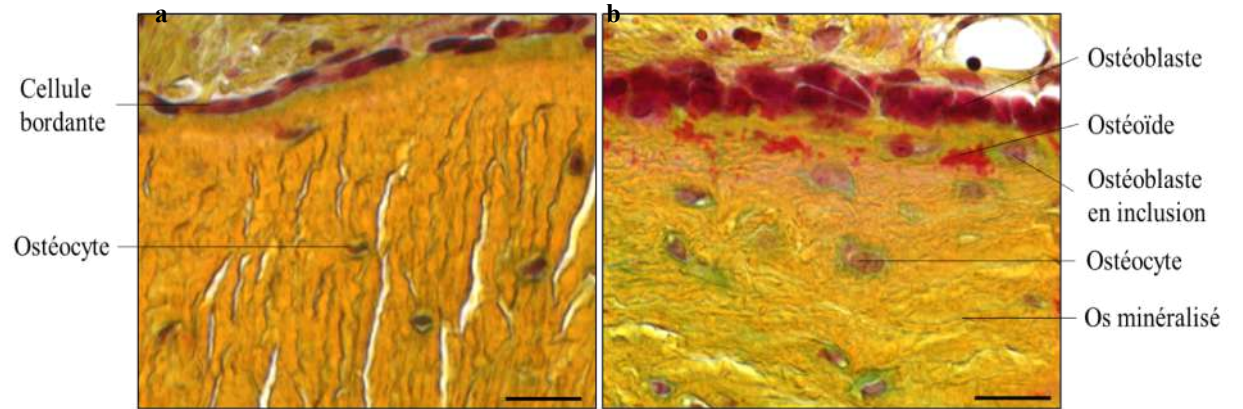


Figure 3 : Observation histologique de tissu osseux. Coloration au pentachrome de Movat. Jaune : collagène, brun : noyaux cellulaires, rouge : barrière ostéoïde. (a) Tissu osseux stable, (b) tissu osseux en formation. Barres d'échelles : $50 \mu\text{m}$.

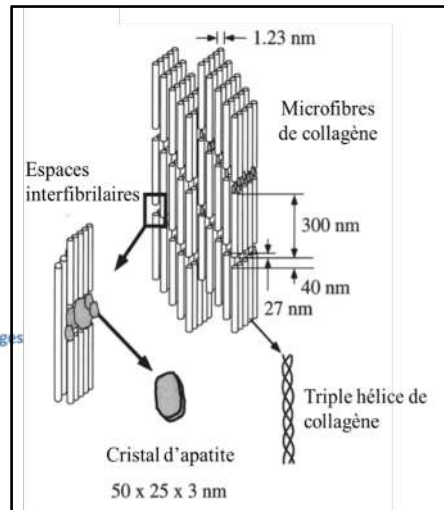


Figure 5 : Organisation submicroscopique de la matrice osseuse[22]

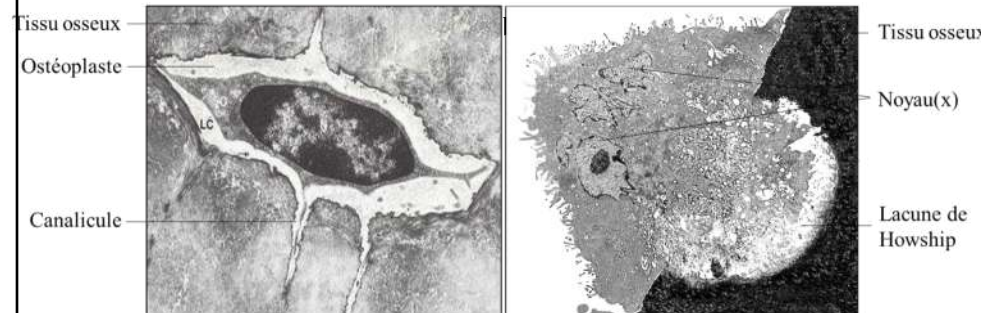


Figure 4 : (a) Observation d'un ostéocyte (généralement $15\text{-}30\mu\text{m}$) dans son ostéoplaste et (b) un ostéoclaste (généralement $50\text{-}100\mu\text{m}$) en activité (Pillet, P./Guicheux, J. non publié). Microscopie électronique à transmission.

La médecine 4R

Replace



On remplace un organe par un objet qui rétablit une fonction : Mécanique et DM

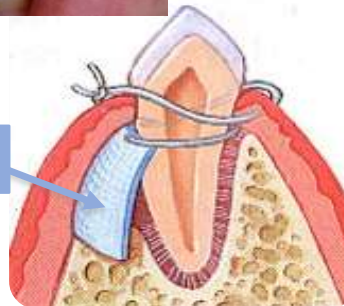
Repair



On répare une partie d'un organe avec un biomatériau bioactif pour rétablir une fonction mécanique et biologique
Matériaux osteo-conducteur

Regenerate

Membrane



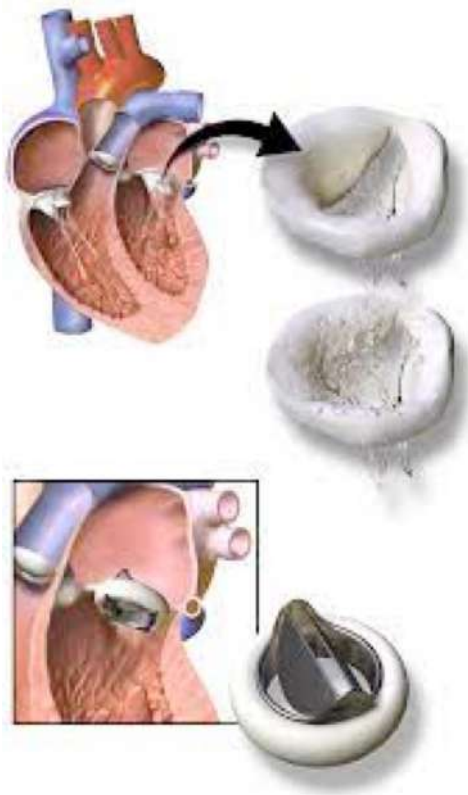
On régénère *ad integrum* une partie d'un organe avec un biomatériau, des cellules, des facteurs de croissance...

Reprogram

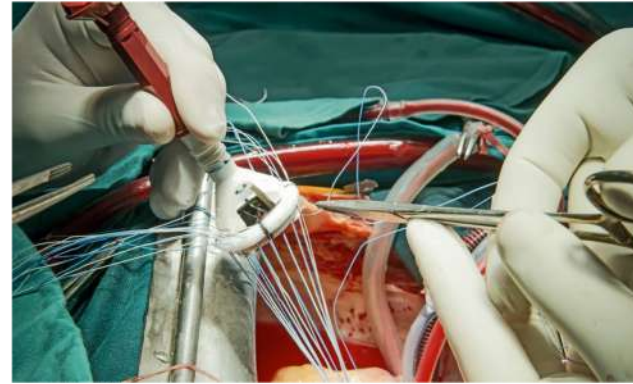


On reprogramme des cellules pour leur demander la régénération d'un tissu.
(Production de FC, IPS (cellules souches pluripotentes induites...))

Remplacer ou réparer ?



On répare le cœur
On remplace une valve ?



On remplace le cœur

Remplacer ou réparer ?

- On répare une partie d'un organe
- On remplace un organe
- Pour retrouver une fonction biologique



REGENERATION

On régénère *ad integrum* une partie d'un organe
avec un biomatériau, des cellules, des facteurs de croissance...

Remodelage osseux

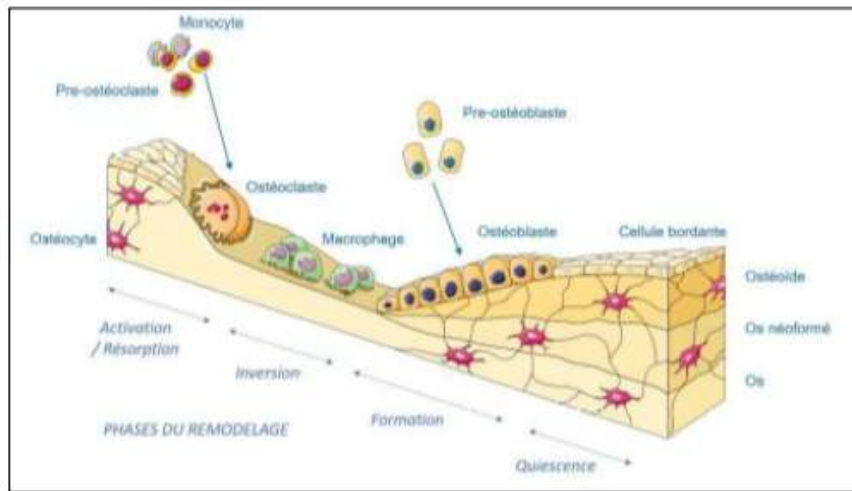


Figure 8 : Cycle du remodelage osseux (adaptée de la banque d'image SERVIER)

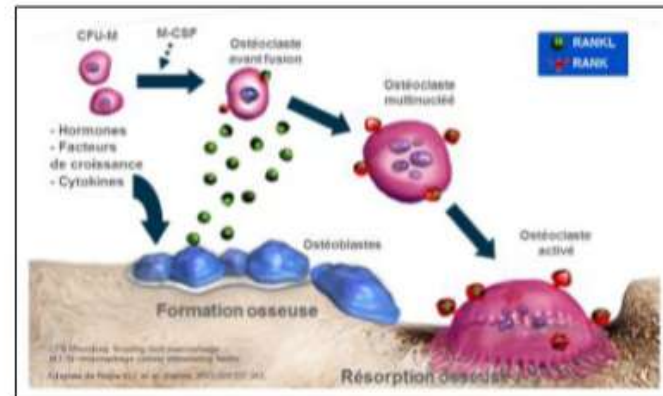


Figure 7 : Activation des ostéoclastes par les ostéoblastes par la sécrétion de différents facteurs solubles (M-CSF et RANK) (44).

La régénération osseuse spontanée

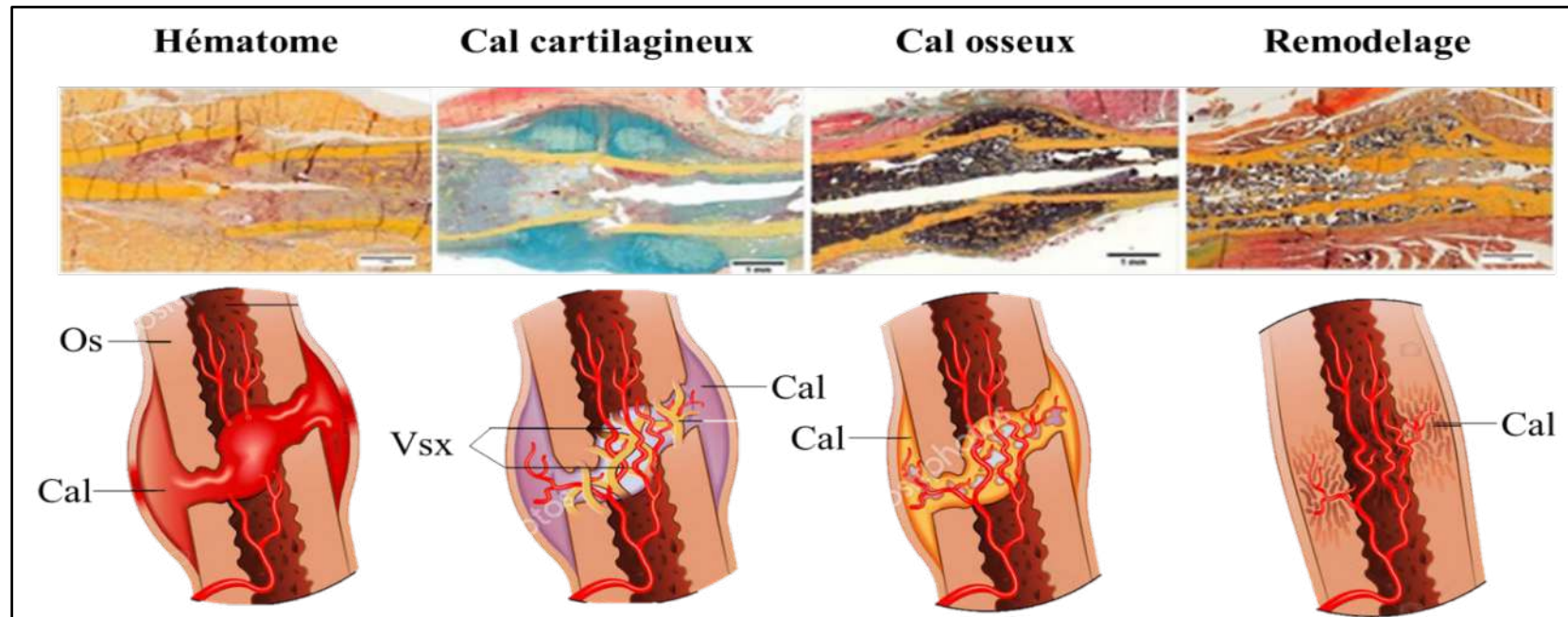


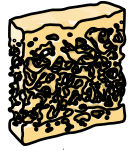
Figure 6 : Les grandes étapes de la régénération osseuse endochondrale. Vsx : vaisseaux sanguins. Modifié d'après Eweida AM, Arch Orthop Trauma Surg. 2012

Limites actuelles de la greffe autologue

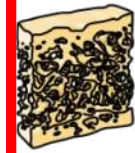
- Taux d'échec de la GO
 - Enfant : 0%
 - Adulte: 10%
- Morbidité tibiale
 - Douleur: 5 jours
 - Boiterie: 10 jours
 - Cicatrice visible: 13%



Corre P *et al.* Intérêt du site de prélèvement tibial médio-proximal dans l'alvéoloplastie secondaire: expérience de 55 cas chez l'enfant. *Rev Stomatol Chir Maxillofac.* 2011 Nov;112(5):280-5



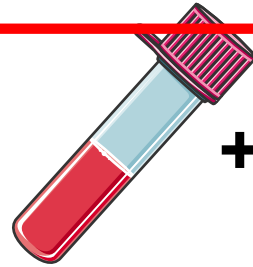
Greffe osseuse = Gold standard



+



Expansion osseuse :
Greffe + Biomatérial



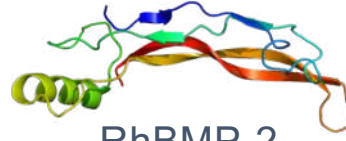
+



Moelle osseuse totale +
Biomatérial



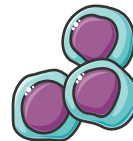
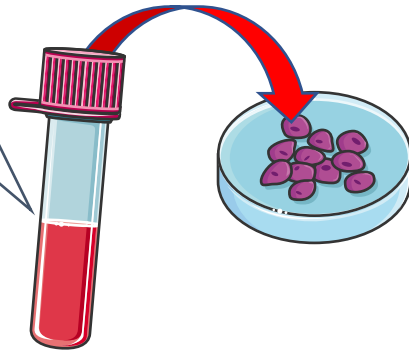
+



RhBMP-2



Pr. Pierre Corre



+/-



Thérapie cellulaire / ITO

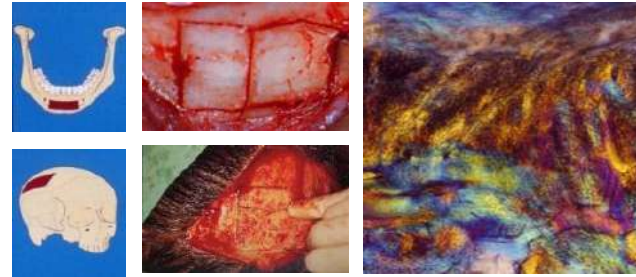
ALTERNATIVES AUX GREFFES

- BIOMATERIAUX
 - Petites cavités
 - Diffusion des protéines et migrations des cellules hôtes dans le matériaux.
 - Adhésion cellulaire puis remodelage
- INGÉNIERIE TISSULAIRE
 - Grosses pertes de substances
 - Cellules du patient multipliées *in vitro*
 - Réimplantées

Biomatériaux pour la régénération osseuse

❑ Autogenous bone (Gold Standard)

- Stock d'os limité (petits paquets)
- Risques de morbidité élevés
- Dououreux et non esthétique



❑ Allograft (Human)

❑ Xenograft bone (Animal)

- Infection (bactérienne - virale)
- Les os morts limitent la prolifération des cellules
- Exigences légales (origines biologiques)



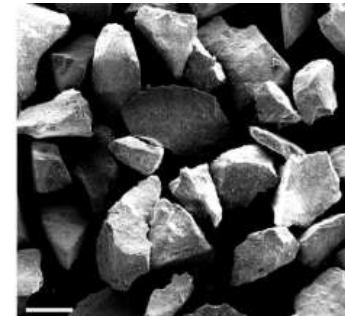
❑ Phosphates de calcium

- Grande variété sur le marché
- Qualité et résultats cliniques différents
- Savoir-faire de production très spécifique



❑ Bio VERRE

- Matériau synthétique contrôlé
- Capable de recruter des cellules ostéoprogénitrices, les "cellules souches" de l'os.
- contrôle le cycle des ostéoblastes pour favoriser la prolifération et la différenciation



Le design des Biomatériaux

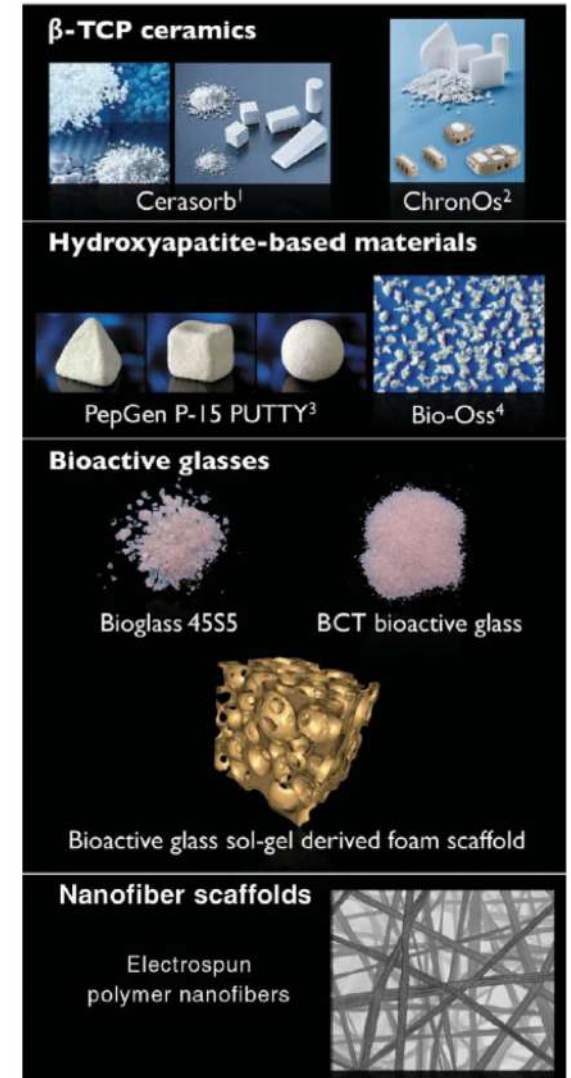
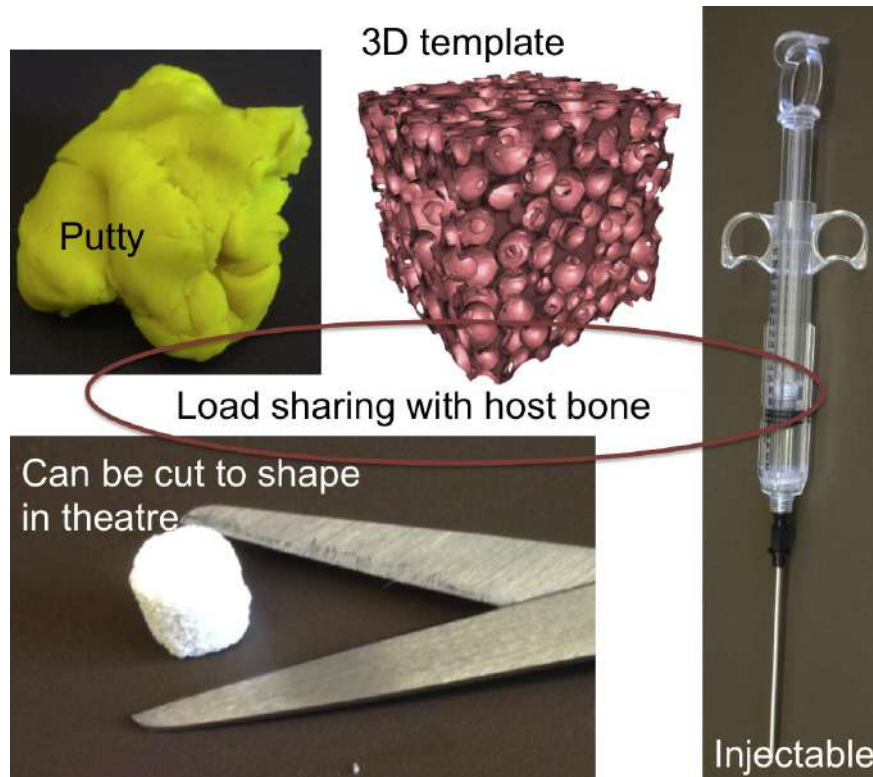


Fig. 2. Macromorphology of some examples of different bone graft materials. (Reproduced with permission from ¹Curasan AG, ²Synthes, ⁴Geistlich. ³Courtesy of Dentsply Tulsa Dental Specialties. © PepGen® P-15.)

Acta Biomaterialia 11 (2015) 103–102

Contents lists available at ScienceDirect

Acta Biomaterialia

journal homepage: www.elsevier.com/locate/actabiomat



Review

Reprint of: Review of bioactive glass: From Hench to hybrids

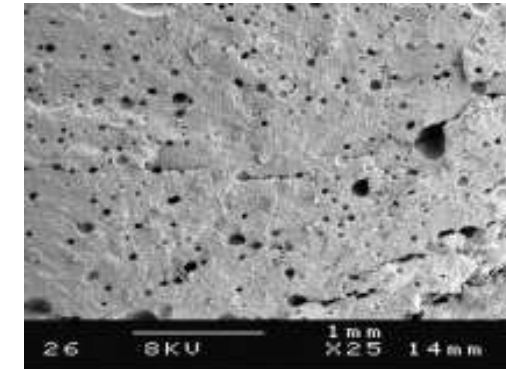
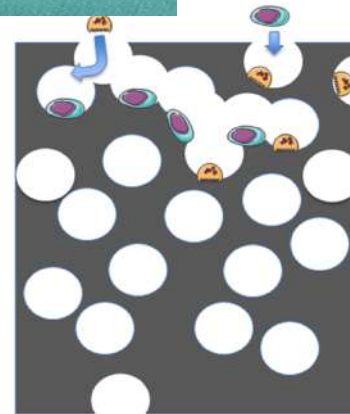
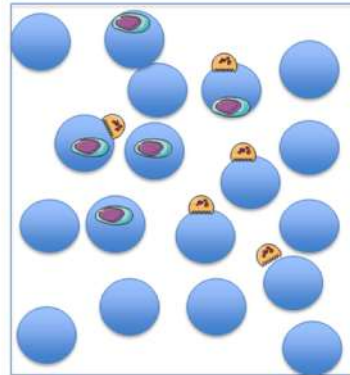
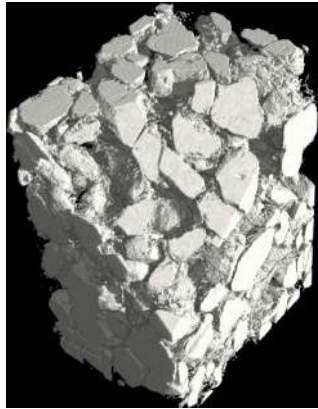
Julian R. Jones*



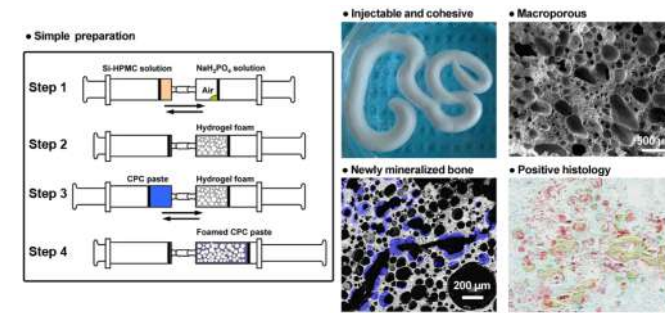
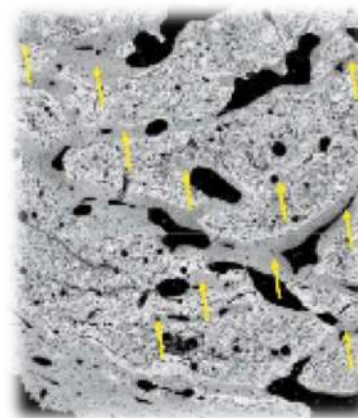
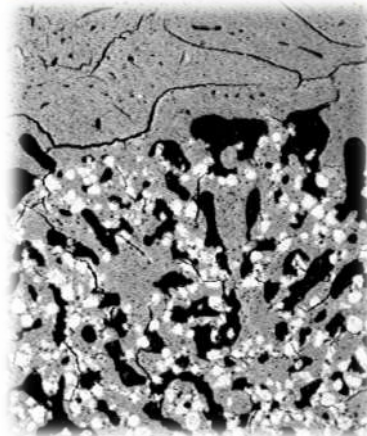
Department of Materials, Imperial College London, South Kensington Campus, London SW7 2BZ, UK



Les Substituts osseux injectables (IBS)



Macroporous and highly resorbable apatitic calcium-phosphate cement
 Khairoun I, Weiss P, Bouler JM
 Application WO2008023254



Available online at www.sciencedirect.com

ScienceDirect

Biomaterials 28 (2007) 3295–3305

Biomaterials

www.elsevier.com/locate/biomaterials

The safety and efficacy of an injectable bone substitute in dental sockets demonstrated in a human clinical trial

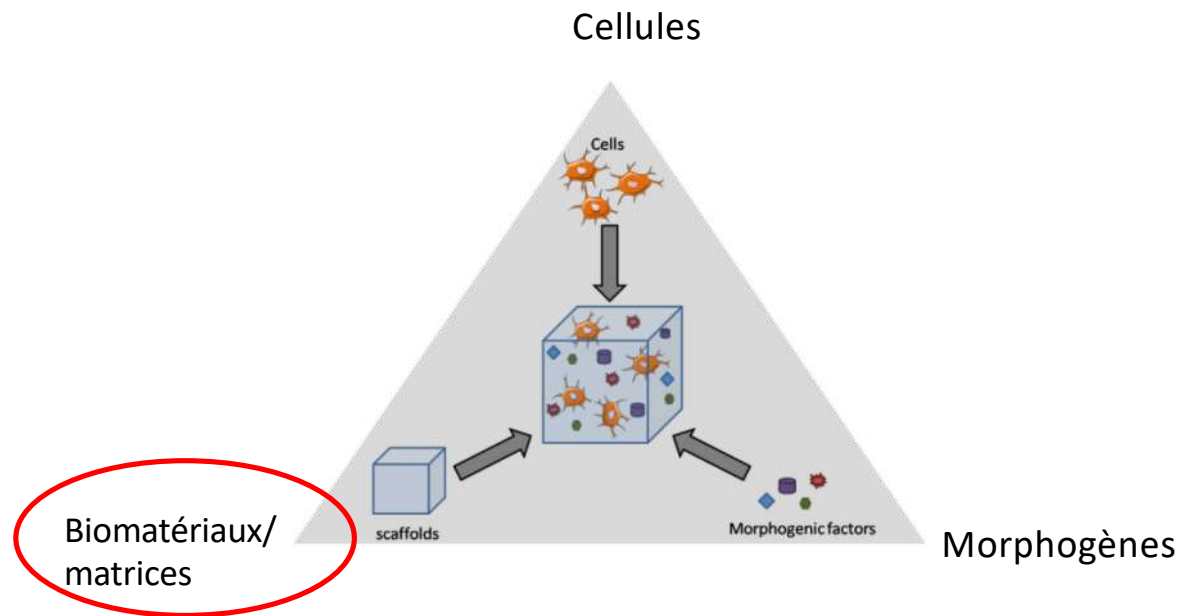
Pierre Weiss^{a,b,c,*}, Pierre Layrolle^{a,b}, Léon-Philippe Clergeau^{b,c}, Bénédicte Enckel^{b,c}, Paul Pilet^{a,c}, Yves Amouriq^{b,c}, Guy Duculs^{a,b}, Bernard Giromelli^{b,c}

Acta Biomaterialia 11 (2015) 129–138
 Contents lists available at ScienceDirect
 Acta Biomaterialia
 journal homepage: www.elsevier.com/locate/actabiomat

Full length article
 A simple and effective approach to prepare injectable macroporous calcium phosphate cement for bone repair: Syringe-foaming using a viscous hydrophilic polymeric solution
 Jingzao Zhang^{a,b,1}, Weizhen Liu^{a,b,1}, Olivier Gauthier^a, Sophie Sourice^a, Paul Pilet^{a,c}, Gildas Rethore^{a,c}, Khalid Khairoun^a, Jean-Michel Bouler^a, Franck Tancet^a, Pierre Weiss^{a,b,c,1,*}

Définition de Ingénierie tissulaire

Un nouveau domaine biomédical regroupant les principes de la biologie cellulaire et du génie biologique, qui permet de reconstruire des structures proches des tissus à partir de cellules vivantes pour des usages in vivo ou ex vivo. Le concept clef en est la reproduction, avec des caractéristiques simplifiées, de l'architecture tissulaire, qui conduit à une intégration immédiate et interactive de ces tissus dans le corps humain (Auger, Canada)



Merceron, Vinatier, Guicheux. Joint Bone Spine 2008
Vinatier, Guicheux. Trends Biotechnol 2009
Vinatier, Guicheux, Noël. Curr Stem Cell Res Ther 2009

Les Apatites Biologiques et synthétiques

le minéral osseux:

- $\text{Ca}_{8,3} (\text{PO}_4)_{4,3} (\text{HPO}_4, \text{CO}_3)_{1,7} (\text{OH}, \text{CO}_3)_{0,3}$

le minéral de l'émail dentaire:

- $\text{Ca}_{9,4} (\text{PO}_4)_{5,4} (\text{HPO}_4, \text{CO}_3)_{0,6} (\text{OH}, \text{CO}_3)_{1,4}$

L'Hydroxyapatite

- $\text{Ca}_{10} (\text{PO}_4)_6 (\text{OH})_2$

Le Phosphate Tricalcique Béta (β -TCP) :

- $\text{Ca}_3 (\text{PO}_4)_2$

Bio Verre

« un verre est un solide non cristallin présentant le phénomène de transition vitreuse » (Zarzycki 1982)

Selected properties of melt-derived Bioglass 45S5 [60,148].

| Property | Value |
|-------------------------------|--|
| Density | 2.7 g cm ⁻³ |
| Network connectivity | 2.12 |
| Glass transition temperature | 538 °C |
| Onset of crystallization | 677 °C |
| Thermal expansion coefficient | 15.1 × 10 ⁻⁶ °C ⁻¹ |
| Young's modulus (stiffness) | 35 MPa |

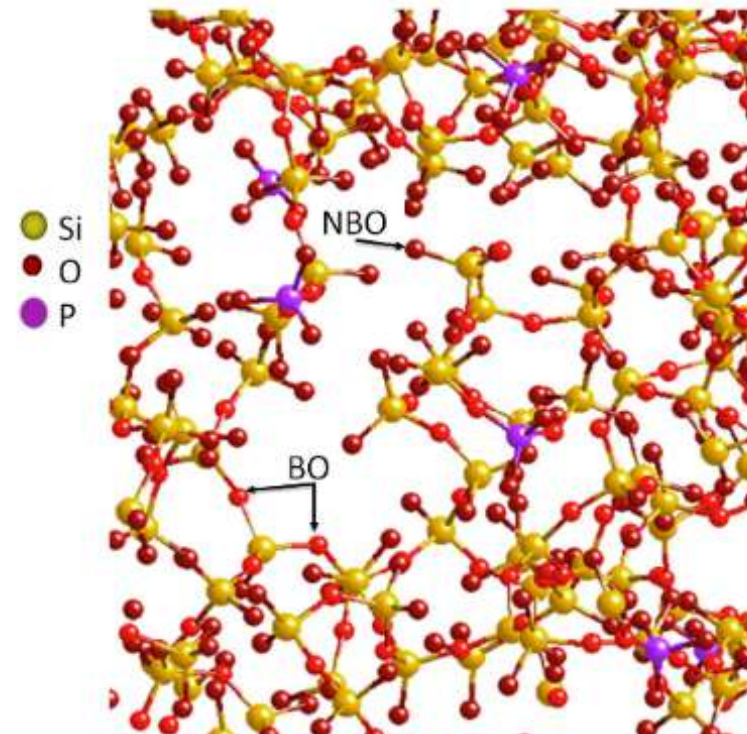


Fig. 10. Section of a model of Bioglass[®] 45S5, with the Na and Ca ions removed for clarity. NBO – non-bridging oxygen, BO – bridging oxygen. Modified from Cormack et al. [136].



Bioglass: 10 milestones from concept to commerce

Larry L. Hench

Department of Biomedical Engineering, Florida Institute of Technology, Melbourne, FL, USA

**Table 1**

Milestones of science and clinical product development of 45S5 Bioglass.

| | |
|------|---|
| 1971 | First publication of bonding of bone to bioactive glasses and glass-ceramics |
| 1981 | Discovery of soft connective tissue bonding to 45S5 Bioglass |
| 1981 | Toxicology and biocompatibility studies (16 in vitro and in vivo) published to establish safety for FDA clearance of bioglass products |
| 1985 | First medical product (Bioglass Ossicular Reconstruction Prosthesis) (MEP) cleared by FDA via the 510 (k) process |
| 1987 | Discovery of osteostimulation in use of Bioglass particulate in regeneration of bone |
| 1988 | Bioglass Endosseous Ridge Maintenance Implant (ERMI) cleared by FDA via the 510 (k) process |
| 1991 | Development of sol-gel processing method for making bioactive gel-glasses extending the bioactive compositional range of bioactivity |
| 1993 | Bioglass particulate for use in bone grafting to restore bone loss from periodontal disease in infrabony defects (PerioGlas) cleared by FDA via the 510 (k) process |
| 1996 | Use of PerioGlas for bone grafts in tooth extraction sites and alveolar ridge augmentation cleared by FDA via the 510 (k) process |
| 2000 | FDA clearance for use of NovaBone in general orthopedic bone grafting in non-load bearing sites |
| 2000 | Quantitative comparison of rate of trabecular bone formation in presence of Bioglass granules versus synthetic HA and A/W glass-ceramic |
| 2000 | Analysis of use of 45S5 Bioglass ionic dissolution products to control osteoblast cell cycles |
| 2001 | Gene expression profiling of 45S5 Bioglass ionic dissolution products to enhance osteogenesis |
| 2004 | FDA clearance of 45S5 particulate for use in dentinal hypersensitivity treatment (NovaMin) |

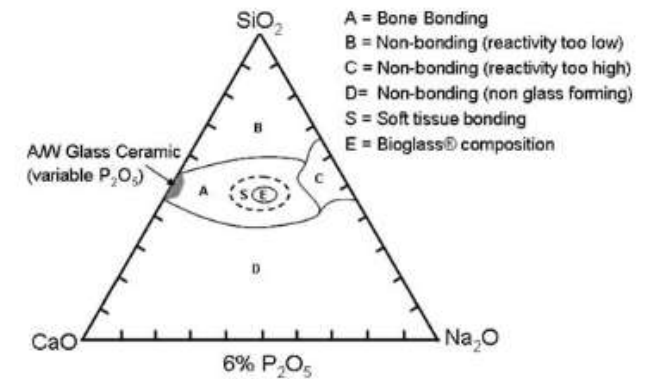


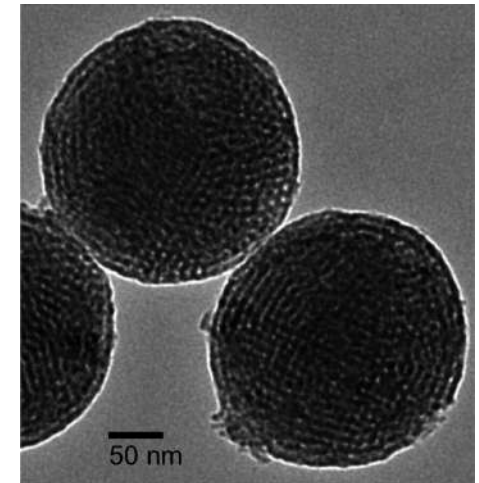
Fig. 1 Compositional diagram for bone-bonding. Note regions A, B, C, D. Region S is a region of Class A bioactivity where bioactive glasses bond to both bone and soft tissues and are gene activating

Différents Bio Verres

- Taille des particules: Micro à nanométriques
- Compositions : avec Argent, Potassium, Magnésium, Strontium...
- Nano ou meso porosité
- +/- Cristallisés

Table IV. Composition of Bioactive Glasses and Glass-Ceramics (wt%)

| Component | 45S5 Bioglass® | 45S5.4F Bioglass® | 45B15S5 Bioglass® | 52S4.6 Bioglass® | 55S4.3 Bioglass® | KGC Ceravital® | KGS Ceravital® | KGy213 Ceravital® | A/W glass-ceramic | MB glass-ceramic | S45P7 |
|--|--------------------------------|----------------------|----------------------|---------------------|---------------------|-------------------|-------------------|----------------------|----------------------|---------------------|-------|
| SiO ₂ | 45 | 45 | 30 | 52 | 55 | 46.2 | 46 | 38 | 34.2 | 19–52 | 45 |
| P ₂ O ₅ | 6 | 6 | 6 | 6 | 6 | | | | 16.3 | 4–24 | 7 |
| CaO | 24.5 | 14.7 | 24.5 | 21 | 19.5 | 20.2 | 33 | 31 | 44.9 | 9–3 | 22 |
| Ca(PO ₃) ₂ | | | | | | 25.5 | 16 | 13.5 | | | |
| CaF ₂ | | 9.8 | | | | | | | 0.5 | | |
| MgO | | | | | | 2.9 | | | 4.6 | 5–15 | |
| MgF ₂ | | | | | | | | | | | |
| Na ₂ O | 24.5 | 24.5 | 24.5 | 21 | 19.5 | 4.8 | 5 | 4 | | 3–5 | 24 |
| K ₂ O | | | | | | 0.4 | | | | 3–5 | |
| Al ₂ O ₃ | | | | | | | | 7 | | 12–33 | |
| B ₂ O ₃ | | | 15 | | | | | | | | 2 |
| Ta ₂ O ₅ /TiO ₂ | | | | | | | | 6.5 | | | |
| Structure | Glass and glass- ceramic | Glass | Glass | Glass | | Glass- ceramic | Glass- ceramic | Glass- ceramic | Glass- ceramic | Glass- ceramic | |



Transmission electron microscope image of ordered mesoporous silica particles. Courtesy of Lijun Ji, Yangzhou University, China.

Synthèse

Fusion : Mélange de matériaux brut inorganiques chauffés entre 1300 et 1600 °C puis refroidi sans permettre la cristallisation

Transformations structurales des bio verres :

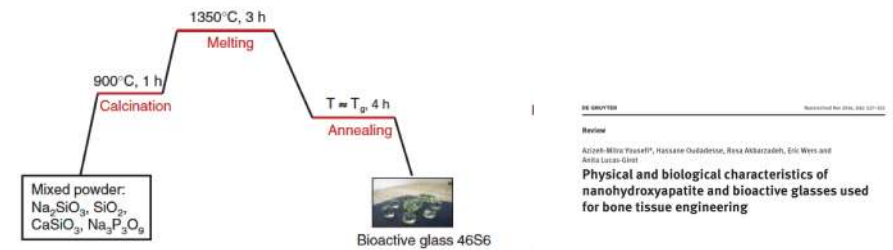
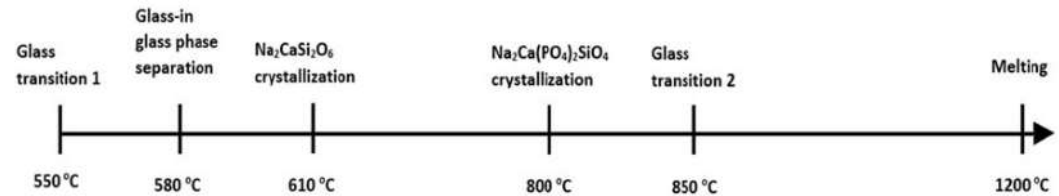
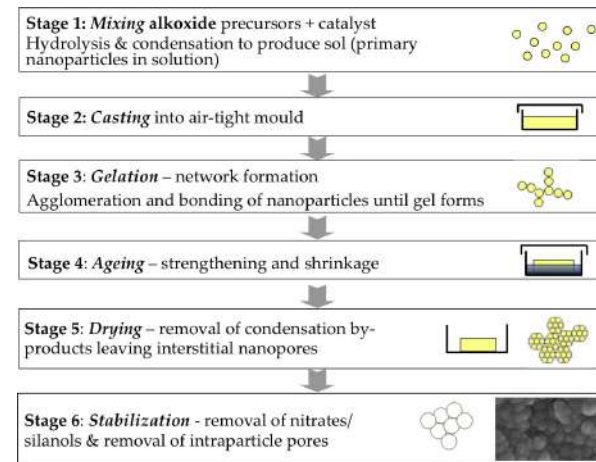


Figure 14 The thermal process for the synthesis of bioactive glass 46S6. Modified from Ref. [138].

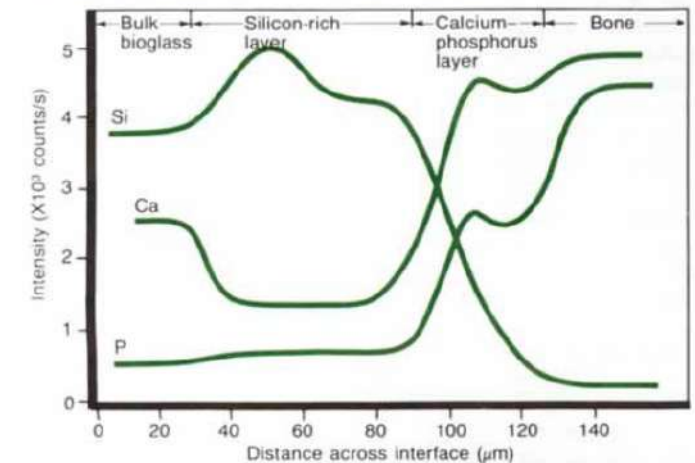
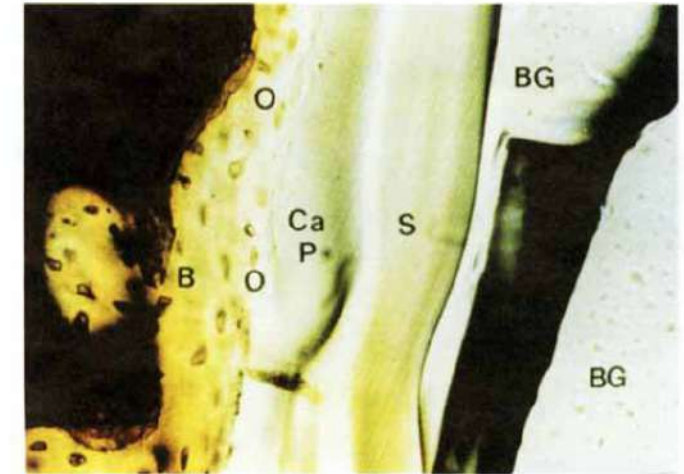
Sol-gel : D'une solution qui gélifie en polymérisant en milieu aqueux. Puis le gel est séché et recuit



A flow chart of the acid-catalysed sol-gel process of synthesis of a bioactive glass with schematics of the evolution of the gel and its nanoporosity.

Interface osseuse

- Une couche d'apatite carbonatée (HCA) bio-active se forme au contact des tissus biologiques à l'interface.
- La phase HCA qui se forme sur les implants bioactifs est chimiquement et structurellement équivalente à la phase minérale de l'os.
- C'est cette équivalence qui est responsable de la liaison interfaciale.



(a) Optical micrograph of a (BG) 4585 Bioglass@ implant bonded to (B) rat bone after 1 year showing (O) osteocytes or bone cells in conjunction with the (Ca-P) HCA layer formed on top of the (S) silica gel (from Ref 44) (b) Electron microprobe analysis across the implant-bone interface shown in (a) (electron microprobe at 20 kV, 100 nA (specimen current), -1- μ m beam diameter, and 20 μ m/(min in) scan rate

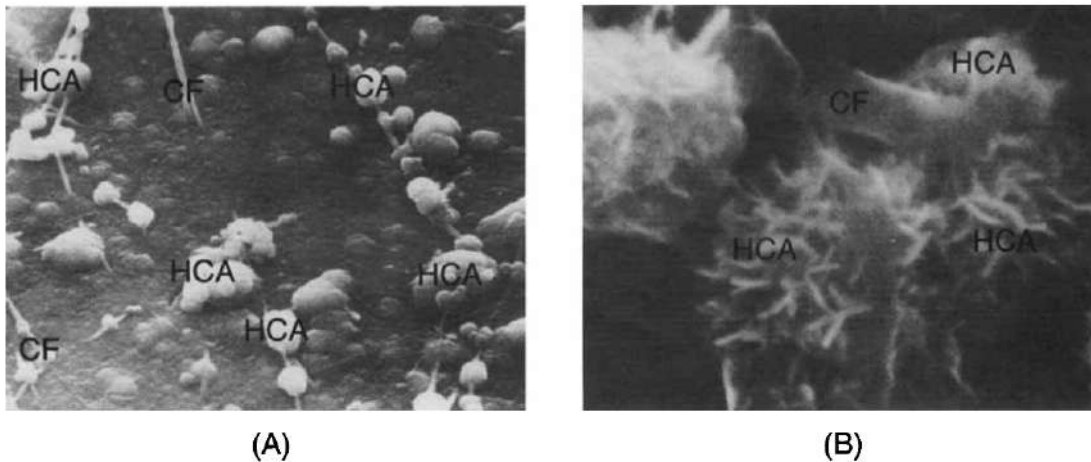
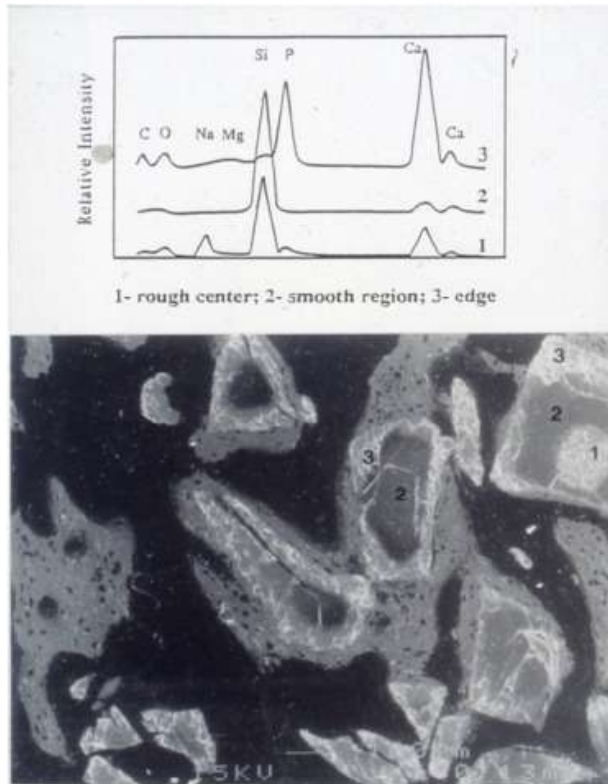
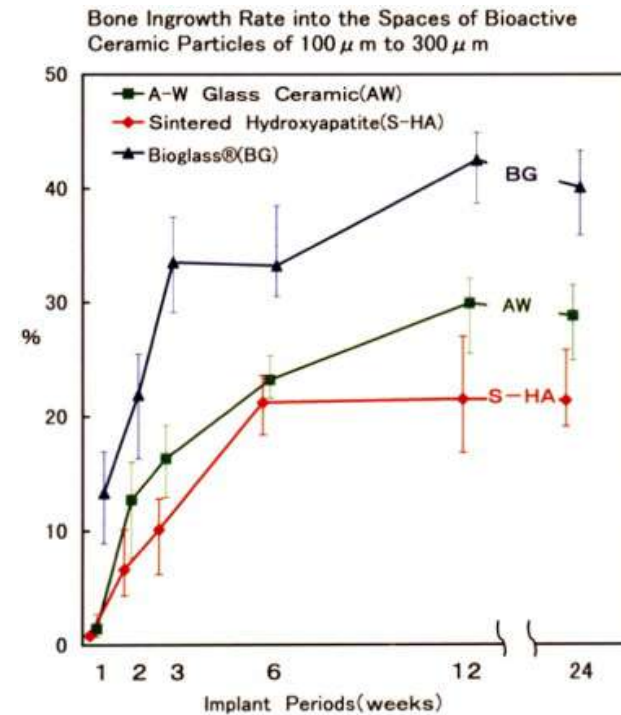


Fig. 9. (a) SEM micrograph of collagen fibrils incorporated within the HCA layer growing on a 45S5 Bioglass® substrate in vitro. (b) Close-up ($\times 11300$) of the HCA crystals bonding to a collagen fibril. (Photographs courtesy of C. Pantano.)

Régénération osseuse avec les Bio Verre

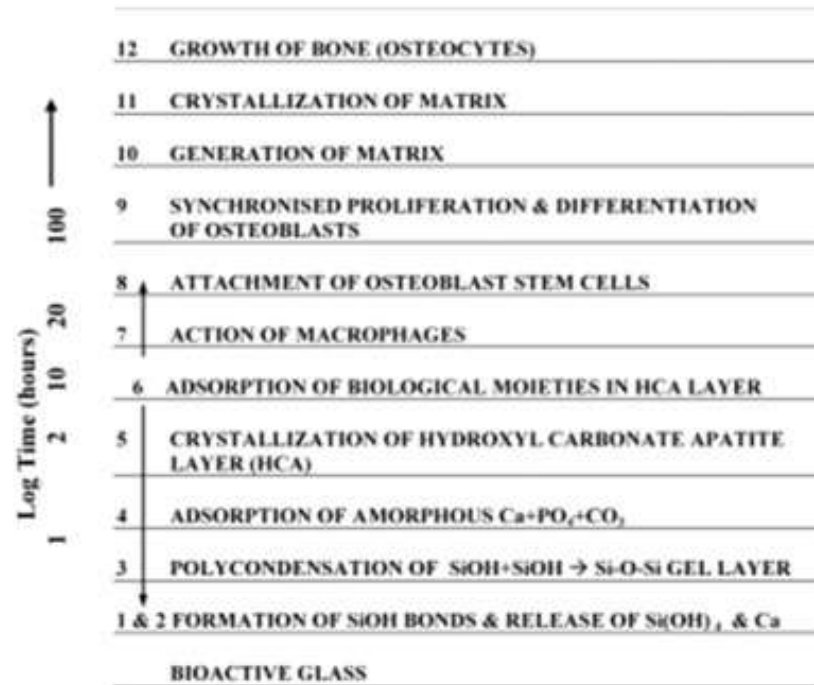


Scanning electron micrograph (SEM) of new bone growing around and connecting 45S5 Bioglass particles to form a regenerated trabecular bone structure. Upper figure is SEM-EDS analysis of the composition gradients of the Bioglass particles due to ion exchange reactions that lead to growth of a biologically active hydroxyl-carbonate-apatite (HCA) layer that is rich in Ca, region #3.

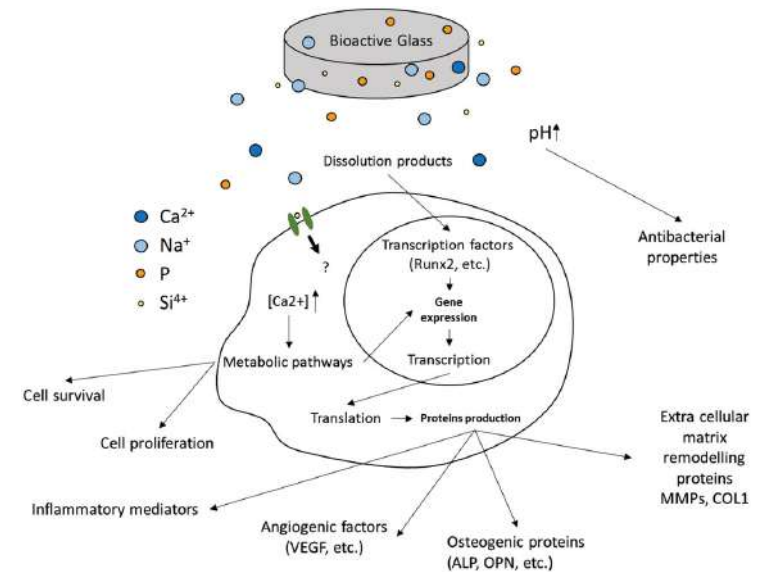


Rapid regeneration of new bone from Class A Bioglass versus Class B bioactive A/W and HA particles in Oonishi critical size defect rabbit condyle model. Note rapid growth of new bone within 4 weeks in the presence of Bioglass particles and eventual greater amount of bone regenerated within the critical size defect.

Effets biologiques des Bioverres



Twelve stages of reaction to form new bone (osteogenesis) bonded to a 45S5 bioactive glass surface. Stages 1–5 are controlled by the kinetics of surface reactions. Note the logarithmic time axis on the left. The early stages of glass surface reactions (Stages 1–4) occur within minutes to a few hours on the most bioactive glass surfaces with compositions ranging from 45 to 52% silica.



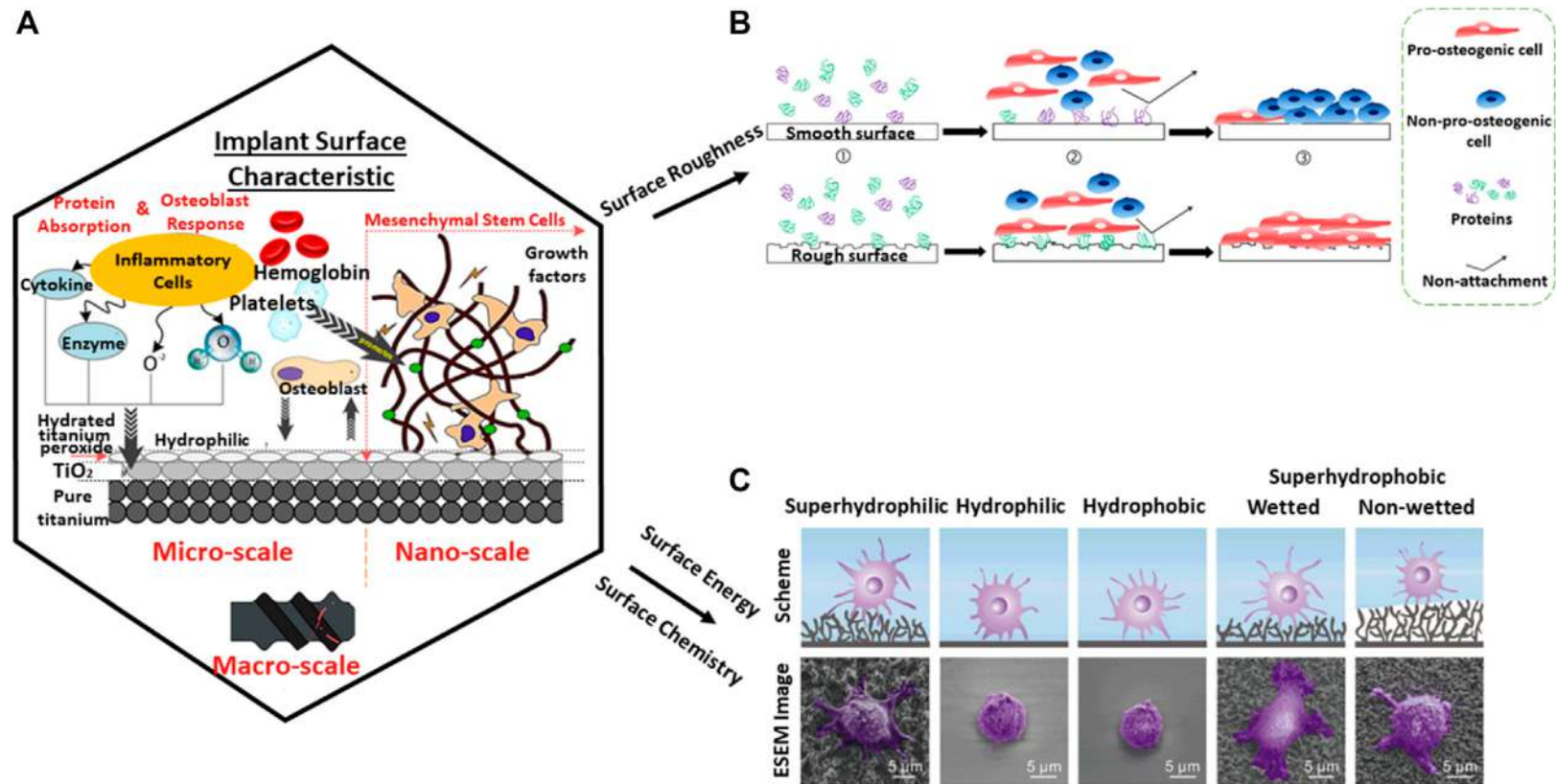
REVIEW

Date: Regeneration

ADVANCED
HEALTHCARE
MATERIALS
www.aahmat.com

Optimized Bioactive Glass: The Quest for the Bony Graft

Henri Granel, Cédric Bossard, Lisa Nucke, Fabien Wauquier, Gael Y. Rochefort, Jérôme Guicheux, Edouard Jallat, Jonathan Lao, and Yohann Wittrant

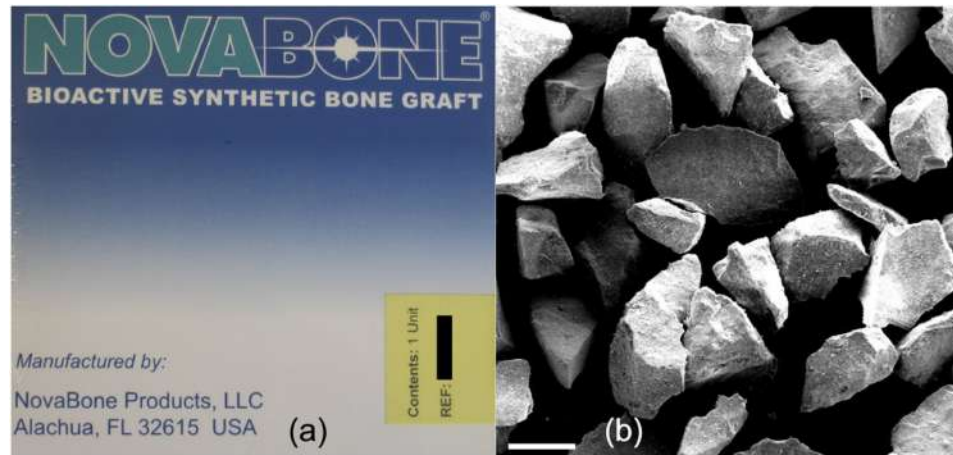


Protein adsorption on the substrate from (A) nano-to-macro level which is dependent on several factors. (B) Surface roughness (Stich et al., 2021). (C) Surface chemistry and surface energy (Meng et al., 2017). Diagram adapted and adjusted from Alipal et al. (2021).

Granules

NORAKER®
THE BIOGLASS® COMPANY

NOVABONE
Proven to Signal, Recruit, Proliferate, and Differentiate.



A) Packaging of NovaBone (45S5 Bioglass) powder for orthopedic applications and (B) scanning electron micrograph of NovaBone particles. Modified with permission from Jones (2013).

IBS

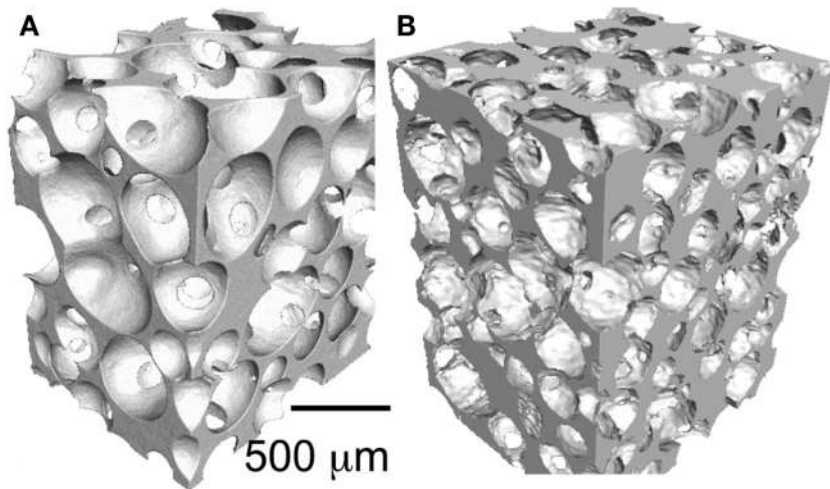


NovaBone Putty is a versatile bone graft substitute that is ready to use out of the package with exceptional handling characteristics that will save time and improve placement.



Glassbone injectable putty is composed of 45S5 bioactive glass and a polymer. This composite technology allows it to be very easily malleable and applicable in complex defects. It is sold directly in the syringe, ready to use.

Mousses de bio verres

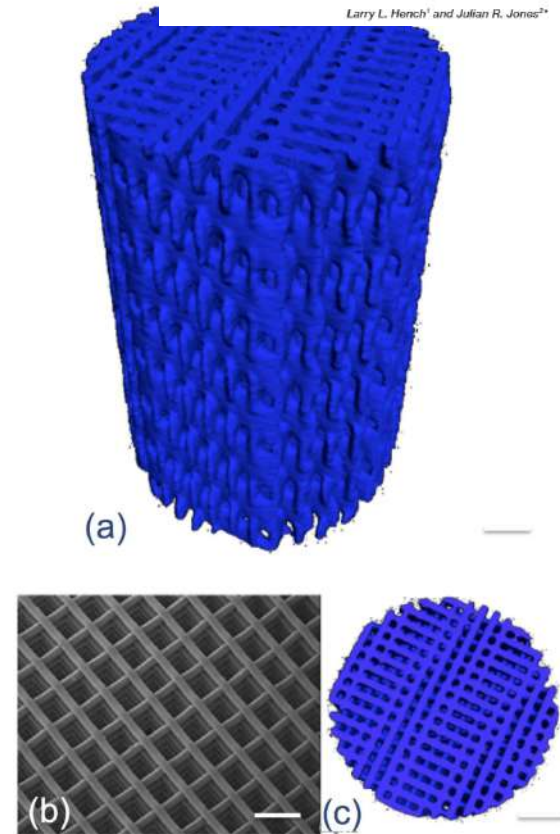


X-ray microtomography images of bioactive glass scaffolds (A) sol-gel foam and (B) melt-derived gel-cast foam. Modified with permission from Jones (2013)

Cependant, les échafaudages en verre bioactif restent fragiles et ne conviennent donc pas à toutes les applications de greffe, comme les sites soumis à des charges cycliques.

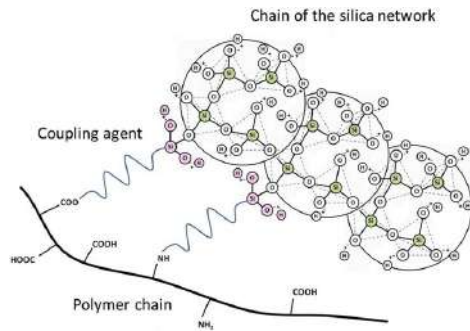
Bioactive Glasses: Frontiers and Challenges

Larry L. Hench¹ and Julian R. Jones^{2*}



X-ray microtomography image of 3-D printed bioactive glass scaffolds. Modified with permission from Jones (2013).

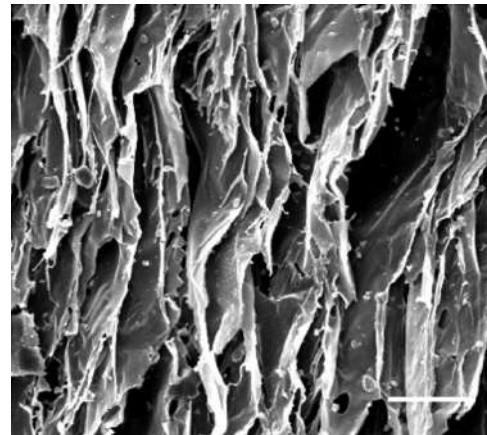
Matériaux hybrides organiques/inorganiques



Granel H. Adv. Healthcare Mater.2019, 8, 1801542



Gelatin/BAG hybrid scaffolds: a) under different shapes; b) observed in scanning electron microscopy. Copyright 2016, The Royal Society of Chemistry (J. Lao, X. Dieudonné, F. Fayon, V. Montouillout, E. Jallot, J. Mater. Chem. B2016, 4, 2486)



An SEM image of a PLLA foam (94% porosity) containing 15vol.% Bioglass 45S5 particles produced by the thermally induced phase separation (TIPS) process. Modified from Blaker et al. 2005 Scale bar is 100μm.

Composites

Table 4
Mechanical characteristics of PLAGA, PCL, and P[3HB] based bioactive glass composite.

| Scaffold | Fabrication Technique | Average Porosity | Mechanical Properties (MPa) | Reference |
|--|---|------------------|---|-----------|
| PLAGA | Traditional solvent casting | 31% | E: 26.48 ± 3.47 ; Compressive Strength: 0.53 ± 0.07 | [130] |
| PLAGA-BG | Traditional solvent casting | 43% | E: 51.34 ± 6.08 ; Compressive Strength: 0.42 ± 0.05 | [130] |
| PLAGA-BG | TIPS | >90% | E: 8-23 | [131] |
| PCL-BG | Particle Leaching/Freeze Extraction | ~ 86% | Compressive Strength: 0.04–0.12; Modulus: 0.45–1.15 | [138] |
| PCL-BG | Solid-Liquid Phase separation | 88–92% | Compressive Strength: 0.092–0.214; Modulus: 0.132–0.251 | [139] |
| PCL-BG | Melt extrusion based Additive manufacturing | ~ 75 | Compressive Young's modulus: 48.35 ± 2.57 | [140] |
| PCL-n SiO ₂ -CaO | Thermal injection Molding | - | Tensile Strength: 19–21.5; Elastic Modulus: 851 ± 43 | [141] |
| PCL- SiO ₂ -CaO-P ₂ O ₅ | Solvent casting | - | Tensile strength = 7–14; Elastic Modulus: 140-170 | [142] |
| PCL-50P ₂ O ₅ +50CaO | Compression molding | - | Flexural strength: 25–30; Modulus (GPa):0.5–2.4 | [143] |
| P[3HB]-BG | Solvent Casting | - | Modulus: 800–1100; Hardness: 120-180 | [144] |

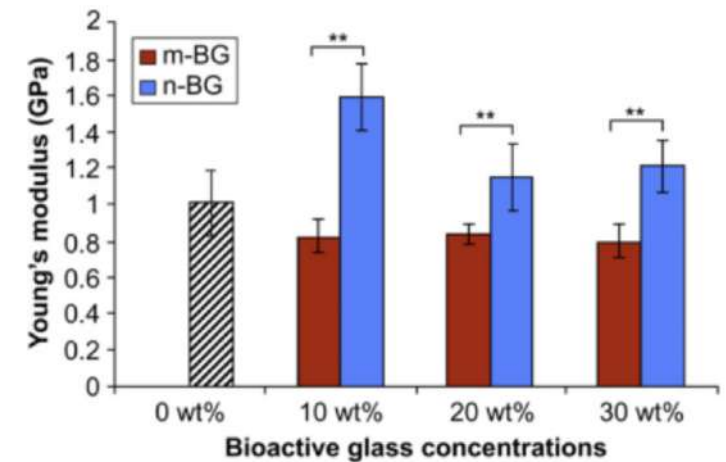
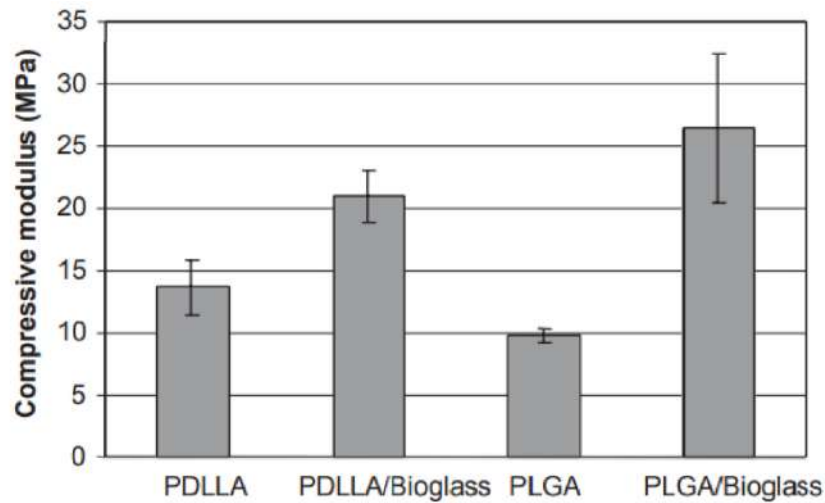


Fig. 5. variation in modulus as change in m-BG and n-BG content in P[3HB]/BG composite [156].

A review on mechanical and In-vitro studies of polymer reinforced bioactive glass-scaffolds and their fabrication techniques

By: Jain, S (Jain, Satish) [1]; Gujjala, R (Gujjala, Raghavendra) [1]; Azeem, PA (Azeem, P. Abdul) [2]; Ojha, S (Ojha, Shakuntala) [3]; Samudrala, RK (Samudrala, Raj Kumar) [2]

View Web of Science ResearcherID and ORCID (provided by Clarivate)

CERAMICS INTERNATIONAL

Volume: 48 Issue: 5 Page: 5908-5921

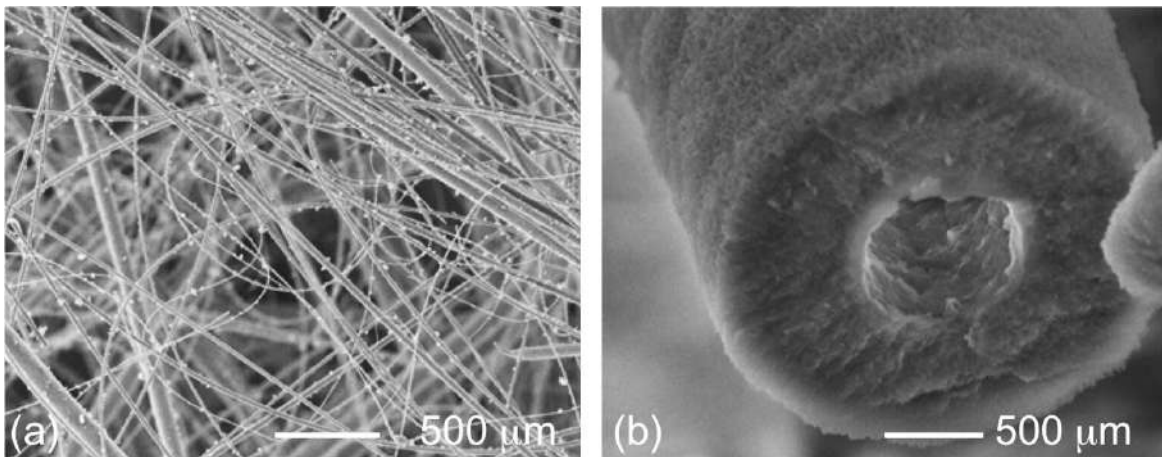
DOI: 10.1016/j.ceramint.2021.11.206

Published: MAR 1 2022

Indexed: 2022-03-02

Document Type: Review

Nano fibres



SEM images of Bioglass 45S5 nanofibres produced by the laser spinning method. (a) The as-produced fibres. (b) After 48h in simulated body fluid a fibre has become a tube of HCA. Modified from Quintero et al.

Acta Biomaterialia 23 (2015) 503–582

Contents lists available at ScienceDirect

Acta Biomaterialia

journal homepage: www.elsevier.com/locate/actabiomat

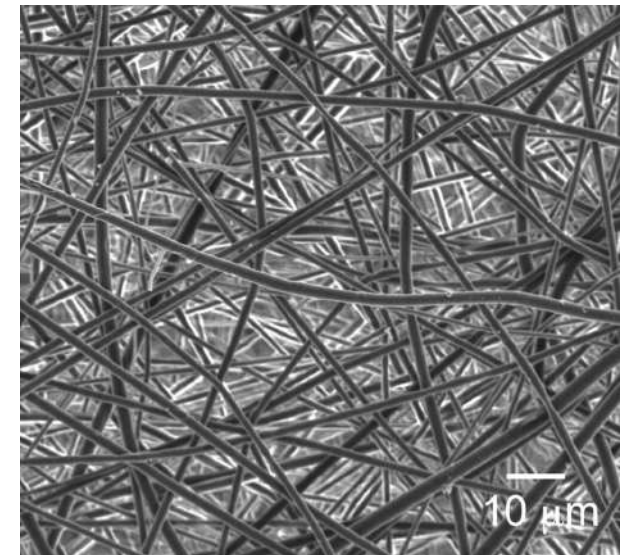
ELSEVIER

Review

Reprint of: Review of bioactive glass: From Hench to hybrids

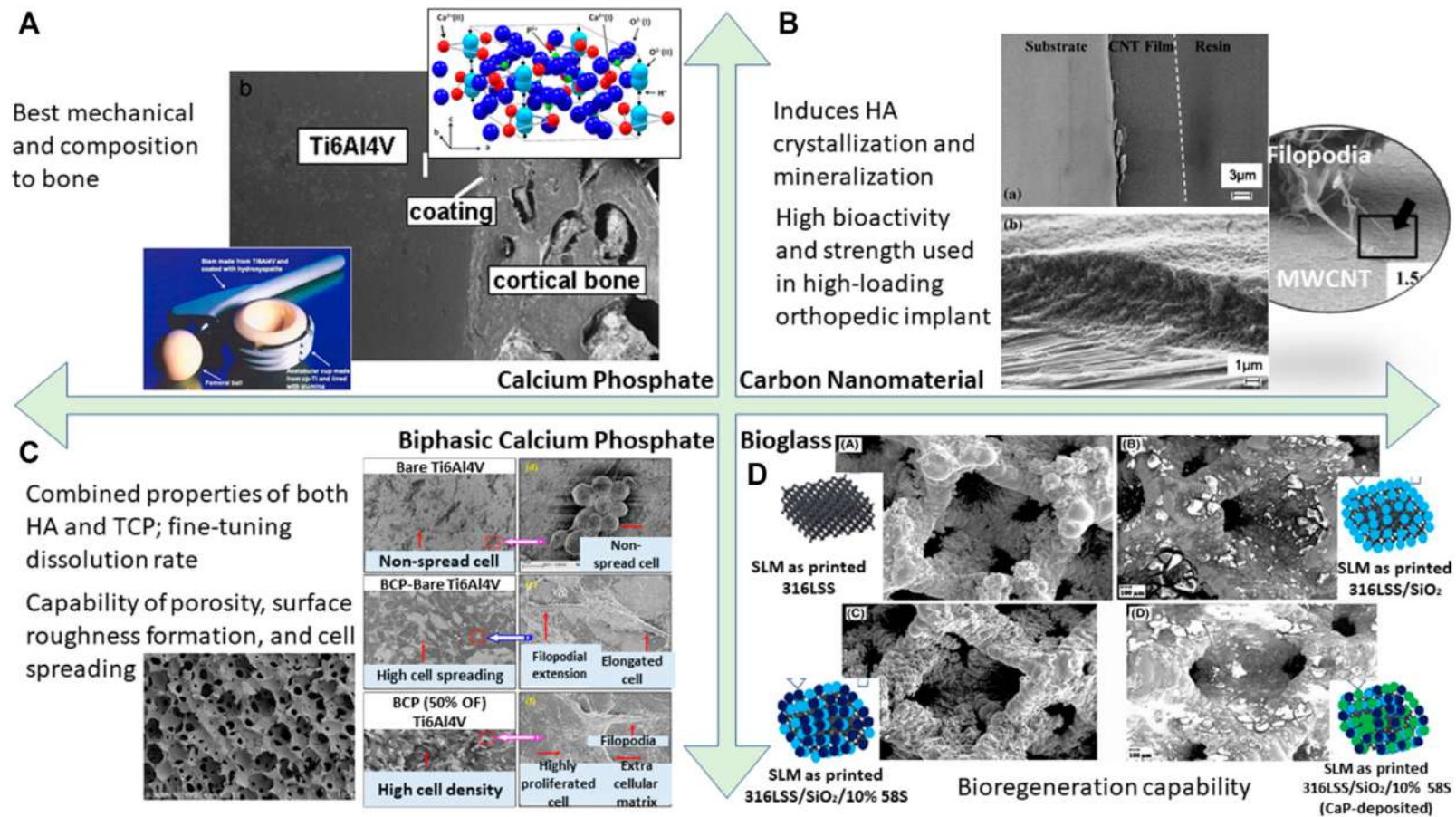
Julian R. Jones*

CrossMark



SEM image of an electrospun sol-gel hybrid fiber mat of silica-calcium-PLLA (20wt.% silica). Courtesy of Gowsihan Poologasundarampillai.

Revêtements



A summary of bioactivity assessment conducted on different types of bioactive coating resulting in cell adhesion capability; (A) calcium phosphate (Heimann 2013). (B) Carbon nanomaterial (Li et al., 2011). (C) Biphasic calcium phosphate (Ebrahimi et al., 2017; Behera et al., 2020). (D) Bioglass (Tabia et al., 2021).

Utilisation clinique

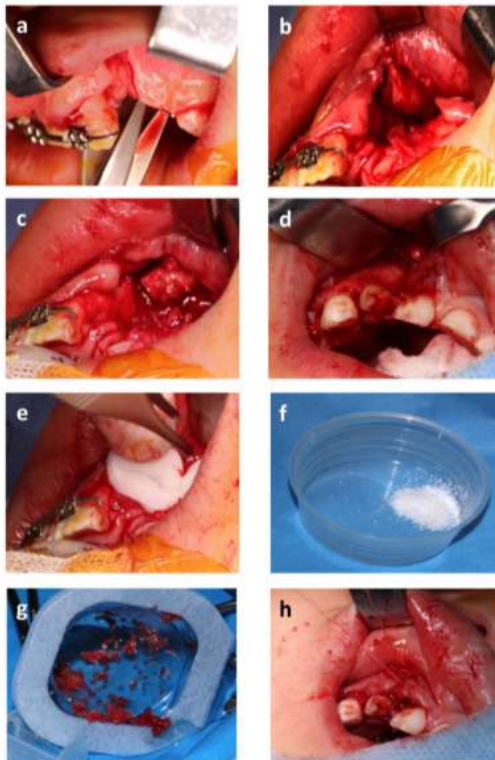
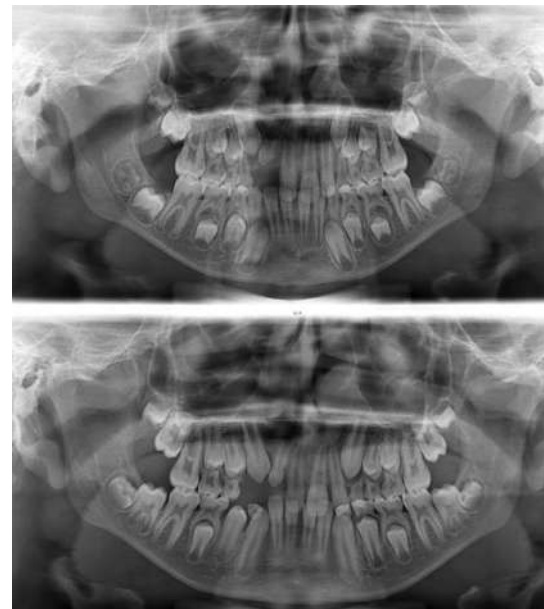


Figure 9: Photographies des étapes de la GOA (d'après la collection personnelle des Drs Audrey Gallucci et Nathalie Degardin, Hôpital La Timone Enfant, AP-HM). (a) Incision de la muqueuse. (b) Lambeau muco-périosté, visualisation du défaut osseux. (c,d) Dissection de la muqueuse nasale. (e) Mise en place du Pangen[®]. (f) GlassBONE[™] pur. (g) GlassBONE[™] mélangé au sang du patient. (h) Sutures finales du lambeau muco-périosté après mise en place du GlassBONE[™].



Dental panoramic view-
preoperative (A) and at 1 year
(B) showing the evolution of the
lateral incisor and the canine
through the right alveolar bone
graft with GlassBONE[™].



Bioactive glass 45S5 ceramic for alveolar cleft reconstruction, about 58 cases²²

Nicolas Graillon ^{1,2,*}, Nathalie Degardin ^{3,4}, Jean Marc Foletti ^{1,2,4}, Magali Seiler ⁵,
Marine Alessandrini ¹, Audrey Gallucci ⁴

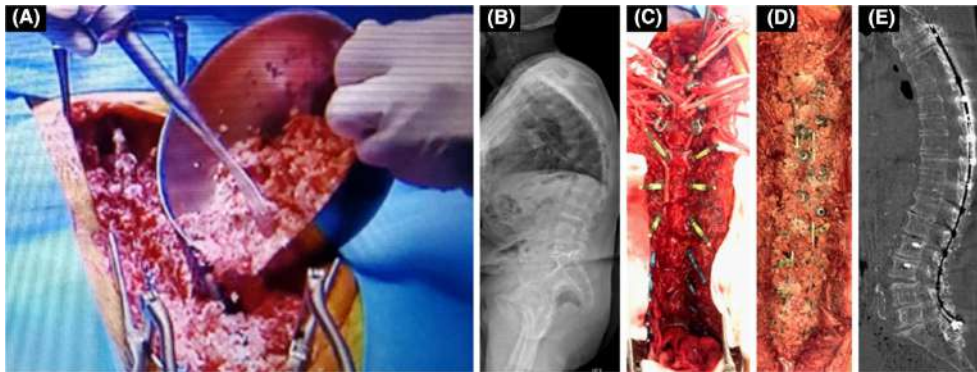
5. Conclusion

Alveolar bone grafting using a synthetic bioactive glass bone substitute can be an alternative to iliac crest bone grafting. It simplifies the surgical procedure and outcomes, allows satisfactory mucosal and bone healing, supports tooth eruption, authorizes the performance of the grafting at an earlier stage, and facilitates the acceptability of a late pre-implant transplant because of its simplicity. In case of failure, it does not contraindicate a new grafting using a bone substitute or autologous bone.



Clinical and radiographic evaluation of bioactive glass in posterior cervical and lumbar spinal fusion

Cédric Barrey¹ · Théo Broussolle¹



Mix of GlassBone with local autologous bone and saline serum place on the decorticated posterior elements of the spine;

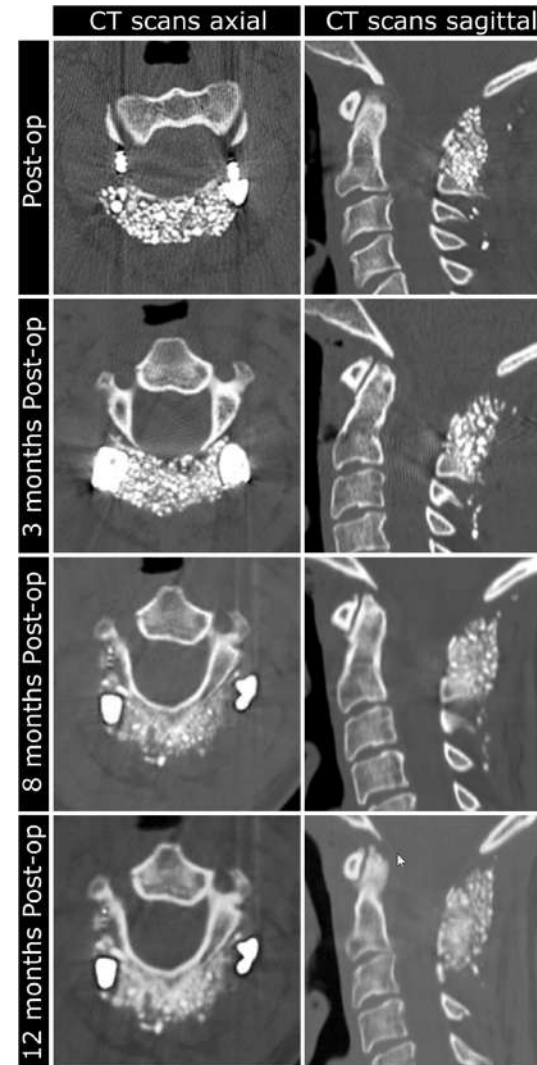


Table 4 Graft consolidation for 29 patients. One patient was excluded for this study (see Table 3)

| Graft consolidation | 12 m post-op cervical (n) | 1 y post-op for T-L-S (n) |
|---------------------|------------------------------|---------------------------------|
| Acquired | 2 (100%) | 22 (82%) |
| In progress | 0 | 3 (11%) |
| Pseudarthrosis | 0 | 2 (7%) |
| Mediocre | 0 | 0 |

T-L-S thoraco-lumbar-sacral

Tissus mous



Review

Bioactive glasses beyond bone and teeth: Emerging applications in contact with soft tissues



Valentina Miguez-Pacheco^a, Larry L. Hench^b, Aldo R. Boccaccini^{a,c,*}

^aInstitute of Biomaterials, University of Erlangen-Nuremberg, 91058 Erlangen, Germany
^bDepartment of Biomedical Engineering, Florida Institute of Technology, Melbourne, FL, USA
^cDepartment of Materials, Imperial College London, London SW7 2AZ, UK

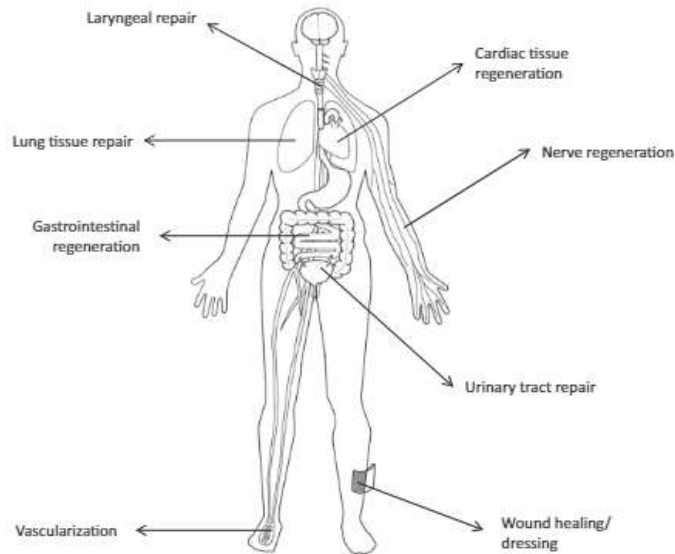
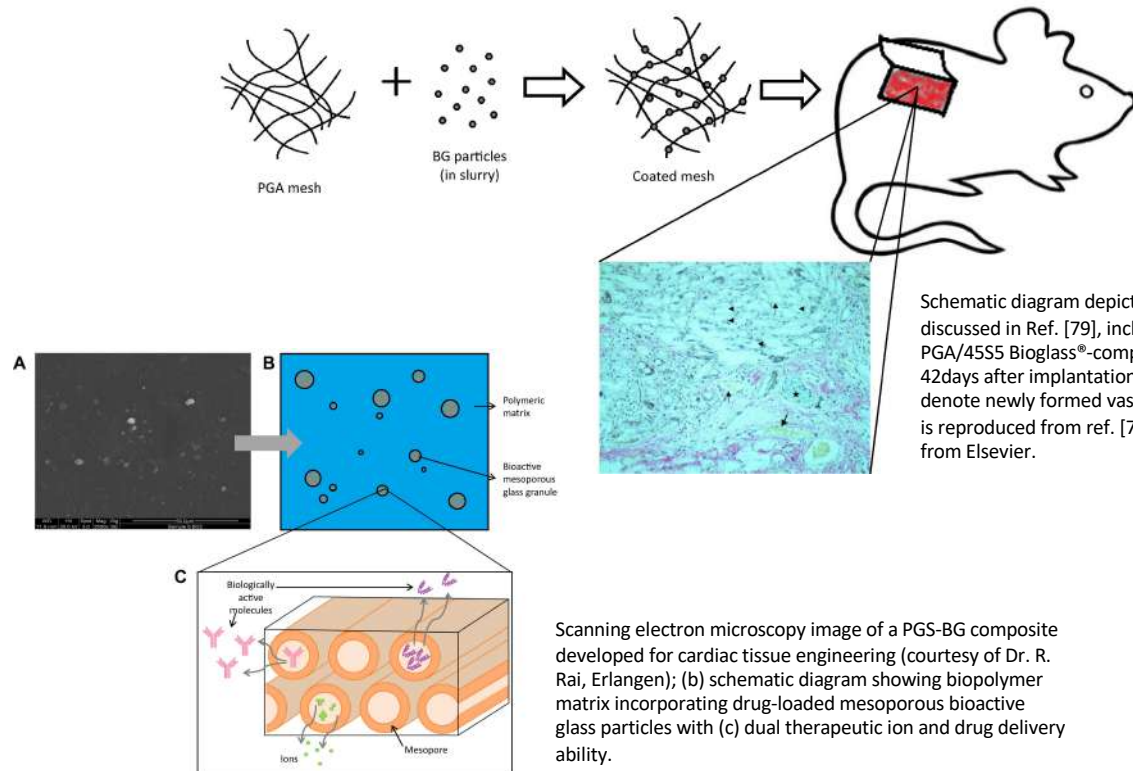


Fig. 1. Schematic diagram indicating emerging BG applications in soft tissue regeneration.



Schematic diagram depicting the experiment discussed in Ref. [79], including the image of PGA/45S5 Bioglass®-composite scaffold 42days after implantation in rat. The arrows denote newly formed vasculature. The image is reproduced from ref. [79] with permission from Elsevier.

Scanning electron microscopy image of a PGS-BG composite developed for cardiac tissue engineering (courtesy of Dr. R. Rai, Erlangen); (b) schematic diagram showing biopolymer matrix incorporating drug-loaded mesoporous bioactive glass particles with (c) dual therapeutic ion and drug delivery ability.

Peau et bio verres

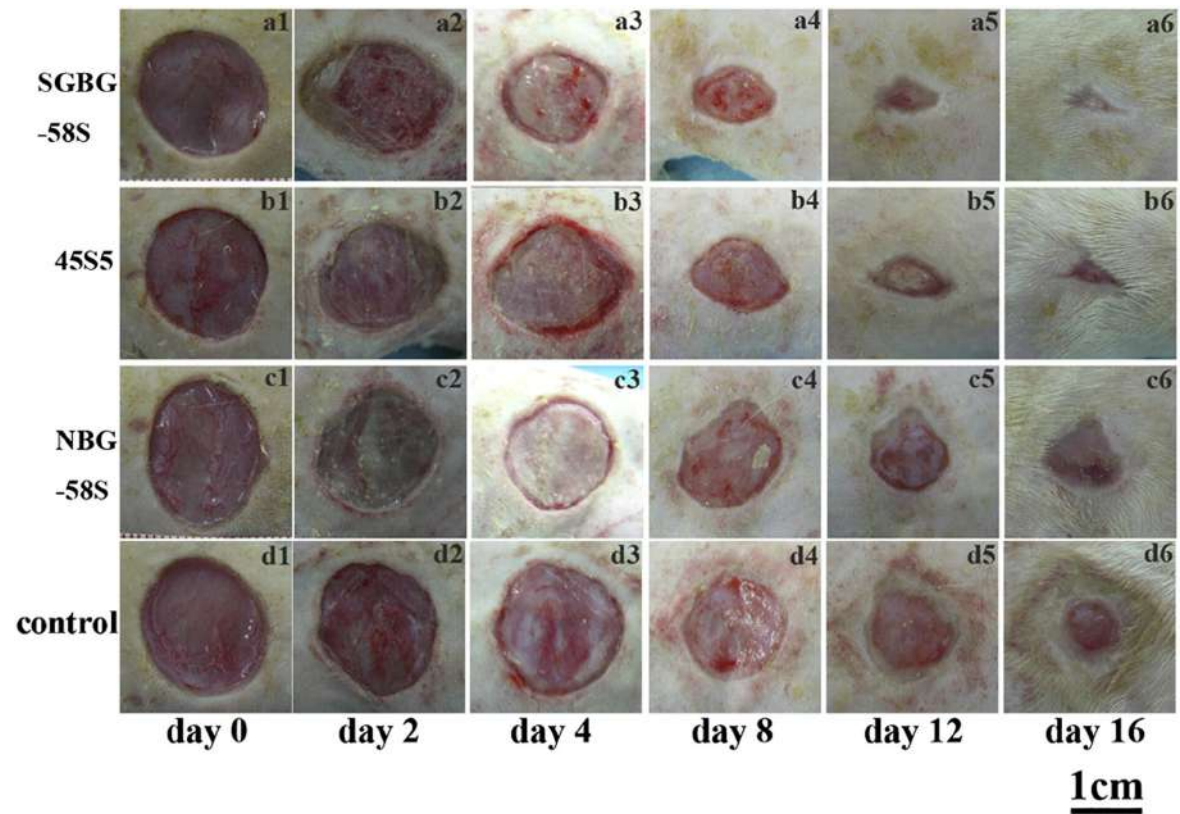
Review

Bioactive glasses beyond bone and teeth: Emerging applications in contact with soft tissues



Valentina Miguez-Pacheco^a, Larry L. Hench^b, Aldo R. Boccaccini^{a,c,*}

^aInstitute of Biomaterials, University of Erlangen-Nuremberg, 91058 Erlangen, Germany
^bDepartment of Biomedical Engineering, Florida Institute of Technology, Melbourne, FL, USA
^cDepartment of Materials, Imperial College London, London SW7 2BZ, UK



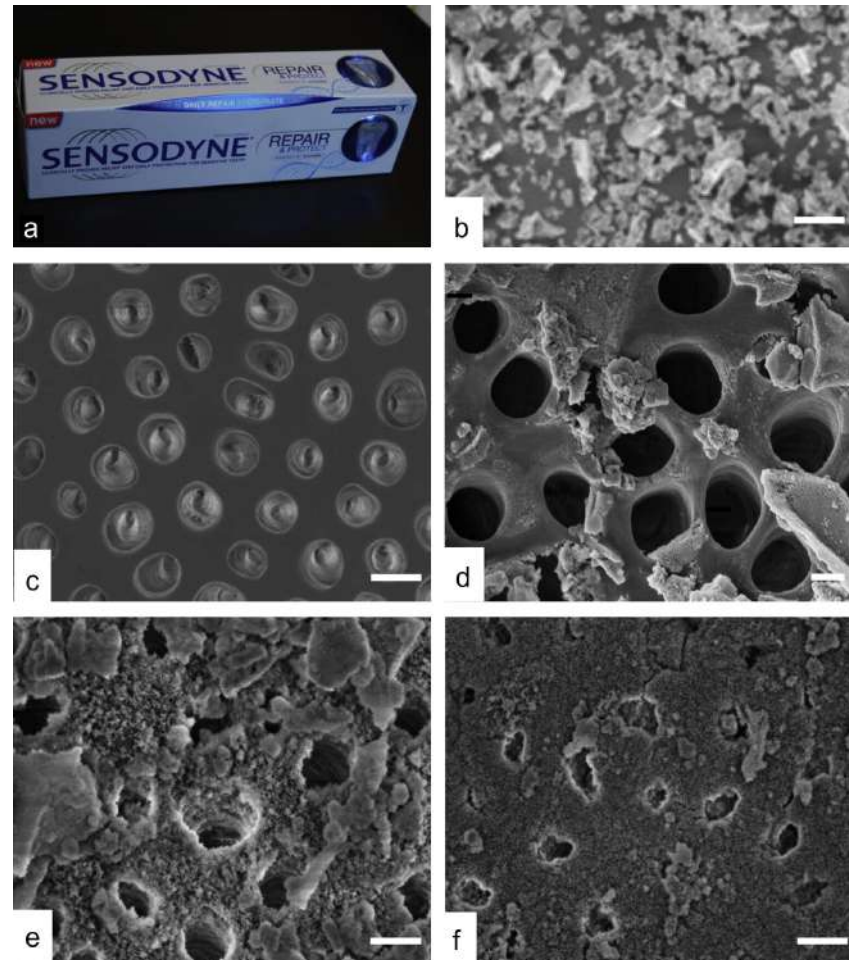
BG treated and untreated wounds from days 0–16 according to Lin et al. [114]. Wounds were treated with different types of BGs, as indicated. It can be seen that SGBG-58S led to the fastest healing rates [114]. Reproduced from ref. [114] by permission of IOP Publishing. All rights reserved.

Lin C, Mao C, Zhang J, Li Y, Chen X. Healing effect of bioactive glass ointment on full-thickness skin wounds. *Biomed Mater* 2012;7(4):045017.

Autres

- Dentifrices

Photograph of Sensodyne Repair and Protect toothpaste, which contains NovaMin[®], a fine particulate of Bioglass 45S5[®]. (b) SEM image of NovaMin particles (bar=20 μ m). (c–f) SEM micrographs of human dentine (bar=1 μ m): (c) untreated, (d) immediately after application of NovaMin in artificial saliva (AS); (e) 24h after application of NovaMin in AS; (f) 5days after application. SEM images modified from Earl et al.



Conclusion

- Bio verres sont des matériaux intéressants et efficaces pour la régénération tissulaire des tissus minéralisés ou non
- Contrairement aux céramiques cristallines de nombreux ions actifs peuvent être ajoutés
- Bioactifs ++
- Nombreux designs d'échafaudages possibles
- Matériaux fragiles et résorbés rapidement

- → adapté pour certaines applications cliniques :
- → Large arsenal thérapeutique